

Recognition of a Mononucleosomal Histone Modification Pattern by BPTF via Multivalent Interactions

Alexander J. Ruthenburg,^{1,7} Haitao Li,^{5,8} Thomas A. Milne,^{1,9} Scott Dewell,² Robert K. McGinty,³ Melanie Yuen,³ Beatrix Ueberheide,⁴ Yali Dou,⁶ Tom W. Muir,³ Dinshaw J. Patel,⁵ and C. David Allis^{1,*}

¹Laboratory of Chromatin Biology and Epigenetics

²Genomics Resource Center

³Laboratory of Synthetic Protein Chemistry

⁴Laboratory of Mass Spectrometry and Gaseous Ion Chemistry

The Rockefeller University, 1230 York Avenue, New York, NY, 10065, USA

⁵Structural Biology Program, Memorial Sloan-Kettering Cancer Center, New York, NY, 10065, USA

⁶Department of Pathology, University of Michigan Medical School, 1301 Catherine Street, Ann Arbor, MI, 48109, USA

⁷Present address: Department of Molecular Genetics and Cell Biology, The University of Chicago, 920 East 58th Street, Chicago, IL 60637, USA

⁸Present address: School of Medicine, Tsinghua University, Beijing 100084, People's Republic of China

⁹Present address: MRC Molecular Haematology Unit, Weatherall Institute of Molecular Medicine, University of Oxford, Headington, Oxford OX3 9DS, UK

*Correspondence: alliscd@rockefeller.edu

DOI 10.1016/j.cell.2011.03.053

SUMMARY

Little is known about how combinations of histone marks are interpreted at the level of nucleosomes. The second PHD finger of human BPTF is known to specifically recognize histone H3 when methylated on lysine 4 (H3K4me2/3). Here, we examine how additional heterotypic modifications influence BPTF binding. Using peptide surrogates, three acetyllysine ligands are identified for a PHD-adjacent bromodomain in BPTF via systematic screening and biophysical characterization. Although the bromodomain displays limited discrimination among the three possible acetyllysines at the peptide level, marked selectivity is observed for only one of these sites, H4K16ac, in combination with H3K4me3 at the mononucleosome level. In support, these two histone marks constitute a unique *trans*-histone modification pattern that unambiguously resides within a single nucleosomal unit in human cells, and this module colocalizes with these marks in the genome. Together, our data call attention to nucleosomal patterning of covalent marks in dictating critical chromatin associations.

INTRODUCTION

The mechanism by which covalent modifications of histones and DNA contribute to the chromatin structural states that govern all DNA-templated processes is a central question to understanding genome management and its dysregulation in human

disease. Advances in understanding the role of chromatin modifications may be divided into two separate veins: (1) enumerating and characterizing chromatin modification-effector pairs (Taverna et al., 2007) and (2) discerning relative modification patterns at the genome level and correlating these patterns to function (Bernstein et al., 2005; Guenther et al., 2007; Wang et al., 2008). However, the convergence of these two areas—how different chromatin binding modules simultaneously engage these modification patterns to transduce downstream function—remains poorly understood.

We have recently proposed that multivalent engagement of nucleosomal units bearing distinct epigenetic signatures by chromatin modification complexes may be involved in many chromatin transactions (Ruthenburg et al., 2007b). Though compelling tests of the “multivalency hypothesis” have yet to occur, earlier studies have provided hints that this phenomenon may be more general than currently appreciated: (1) Greater net binding affinity and substrate specificity beyond the sum of constituent parts may arise in the binding of two proximal acetyllysines in the H4 tail by the bromodomain proteins hTaf1 and Brdt (Jacobson et al., 2000; Morinière et al., 2009); (2) Multiple contact surfaces distributed over a number of subunits (some of which appear to be histone modification dependent) are required for Rpd3S histone deacetylase complex binding to a single nucleosome (Li et al., 2007). However, the interplay between discrete histone modification-dependent interactions has not been well studied in a nucleosomal context, nor is there a clear example of a protein complex or single polypeptide that simultaneously engages two or more histone modifications on a nucleosome for which the discrete constituent interactions are clearly defined. Thus, several key questions posed in the histone code hypothesis (Strahl and Allis, 2000) still remain unresolved: how are combinations of histone modifications

interpreted at the molecular level, are there units of recognition beyond single tails, and what are the functional consequences?

Here, we sought to address how chromatin modification patterns may be simultaneously engaged on the nucleosome level using a PHD finger and adjacent bromodomain of the NURF chromatin remodeling complex subunit BPTF as a paradigm to provide insights into the above questions. We examine the biochemical, structural, and functional properties endowed by a bivalent configuration of these linked effector domains, the simplest case of multivalent histone modification-dependent nucleosomal engagement (Ruthenburg et al., 2007b).

BPTF in the context of the NURF complex is an essential regulator of chromatin structure in development (Badenhorst et al., 2002; Landry et al., 2008; Wysocka et al., 2006), bringing about transcriptional activation or repression in a locus-specific manner (Bai et al., 2007; Kwon et al., 2008) by virtue of the complex's chromatin remodeling activity (Hamiche et al., 1999; Tsukiyama and Wu, 1995). The second PHD finger of BPTF, implicated in recruitment or stabilization of the NURF complex to active homeotic genes as a consequence of MLL1-mediated H3K4 trimethylation, is followed closely by a bromodomain whose mechanistic role is obscure (Wysocka et al., 2006). The spatial coupling of these two domains is sufficiently tight to permit determination of the structure of the terminal PHD-bromodomain module spanned by an apparently rigid linker α helix (Li et al., 2006). Though the molecular details of H3K4me3 binding by the PHD finger are known, the ligand for the associated bromodomain remains unclear. Given that the bromodomain is a well-established histone acetyllysine recognition domain (Dhalluin et al., 1999; Mujtaba et al., 2007), we envisioned that, together with the PHD finger, this bivalent structural element may bind two different classes of histone modifications generally associated with euchromatin and transcription initiation (Guenther et al., 2007; Ruthenburg et al., 2007a; Shogren-Knaak et al., 2006). In support, deletion of both the PHD finger and the adjacent bromodomain rescued BPTF knockdown in *Xenopus* less efficiently than a PHD finger mutation that completely abolishes H3K4me3 interactions (Wysocka et al., 2006). To examine the nature of this putative bivalent nucleosomal recognition by the PHD-bromo module (Figure 1A), we first sought to identify and characterize potential bromodomain binding partners.

RESULTS

The BPTF Bromodomain Binds Three Different Acetylated H4 Peptides

Using SPOT blotting (Nady et al., 2008), we screened a spatially arrayed library of all known core histone acetylation marks (Basu et al., 2009). This analysis revealed two acetylation marks that specifically bound recombinant BPTF bromodomain (Figure 1B). Peptides representing histone H4 acetylated lysines 16 and 20 (H4K16ac and H4K20ac) consistently displayed the strongest interaction with the BPTF bromodomain in this assay, whereas the unmodified counterpart displayed no detectable signal above background (Figure 1B and Figure S1C available online). Affinities for these two peptides and set of control peptides were validated by peptide pull-down and then examined more

carefully via fluorescence polarization anisotropy (FPA) and isothermal titration calorimetry (ITC) (Figures 1C–1E). These additional experiments revealed affinity for H4K12ac, perhaps not apparent with SPOT analysis because the array peptide only included three residues N terminal to the K12ac mark. Quantitative binding measurements lend support to the apparent specificity for these three acetylation sites in the H4 tail, whereas other acetylated H4 peptides and unmodified H4 counterparts displayed only weak affinity outside of the experimentally quantifiable range (Figures 1D and 1E and Figures S1E, S1F, S1G, and S1H). These measurements are consistent with the promiscuity and affinity (H4K12ac [K_d , ITC = $69 \pm 1 \mu\text{M}$], H4K16ac [K_d , ITC = $99 \pm 7 \mu\text{M}$], and H4K20ac [K_d , ITC = $130 \pm 10 \mu\text{M}$]) reported for other bromodomains (Dhalluin et al., 1999; Mujtaba et al., 2007; Zeng et al., 2008).

Properties of BPTF PHD-Bromo Binding at the Peptide versus Nucleosome Level

With a small set of bromodomain binding partners characterized, combined with the well-established PHD finger affinity for H3K4me2/3 (Li et al., 2006; Wysocka et al., 2006), we sought to examine the properties of bivalent ligand binding by these two linked binding domains. Simultaneous binding of the BPTF PHD-bromo cassette could have two nonexclusive consequences: allosteric cooperativity wherein the binding of a given peptide in one of the two modules may influence the binding of cognate peptide to the other by a conformational shift (Changeux and Edelstein, 2005) or a multivalent interaction wherein two coupled entities may bind with greater net affinity and specificity than their discrete constituent binding equilibria, largely as an entropic effect (Krishnamurthy et al., 2006; Ruthenburg et al., 2007b). We used peptide-level binding experiments with the PHD-bromo module exploiting the heterotypic ligand binding properties of each domain with one ligand at saturating concentration to query for possible allosteric enhancement. For simplicity, we restricted our initial experiments to H4K16ac in combination with H3K4me3. The binding of the PHD-bromo unit to a fluorescein-labeled H3K4me3 peptide was assessed by FPA in the presence of unlabeled H4K16ac peptide at a concentration 5-fold greater than its bromodomain binding K_d . This titration did not reveal any significant displacement of the binding curve relative to similar titrations with excess unmodified H4 peptide or without any H4 peptide (Figure 2A). Moreover, the reciprocal experiment did not detect cooperativity (Figure 2B). Thus, we conclude that, at the peptide level, each binding event is free from detectable allostery.

If the binding of both peptides is effectively bimolecular, as might be anticipated for the BPTF PHD-bromodomain engaging both marks within a nucleosome, a free energy enhancement in binding might occur due to multivalency (Krishnamurthy et al., 2006; Ruthenburg et al., 2007b). To test this possibility, we developed a novel biophysical assay with histone peptides attached to a rigid DNA duplex to assess the spatial requirements of cooperative and simultaneous histone tail binding. When the spacing between these two short peptides along one face of the B form DNA duplex is $\sim 71 \text{ \AA}$ (Figure S2A), marked enhancement of PHD-bromodomain binding affinity is observed, relative to DNA-peptide conjugates bearing each single peptide

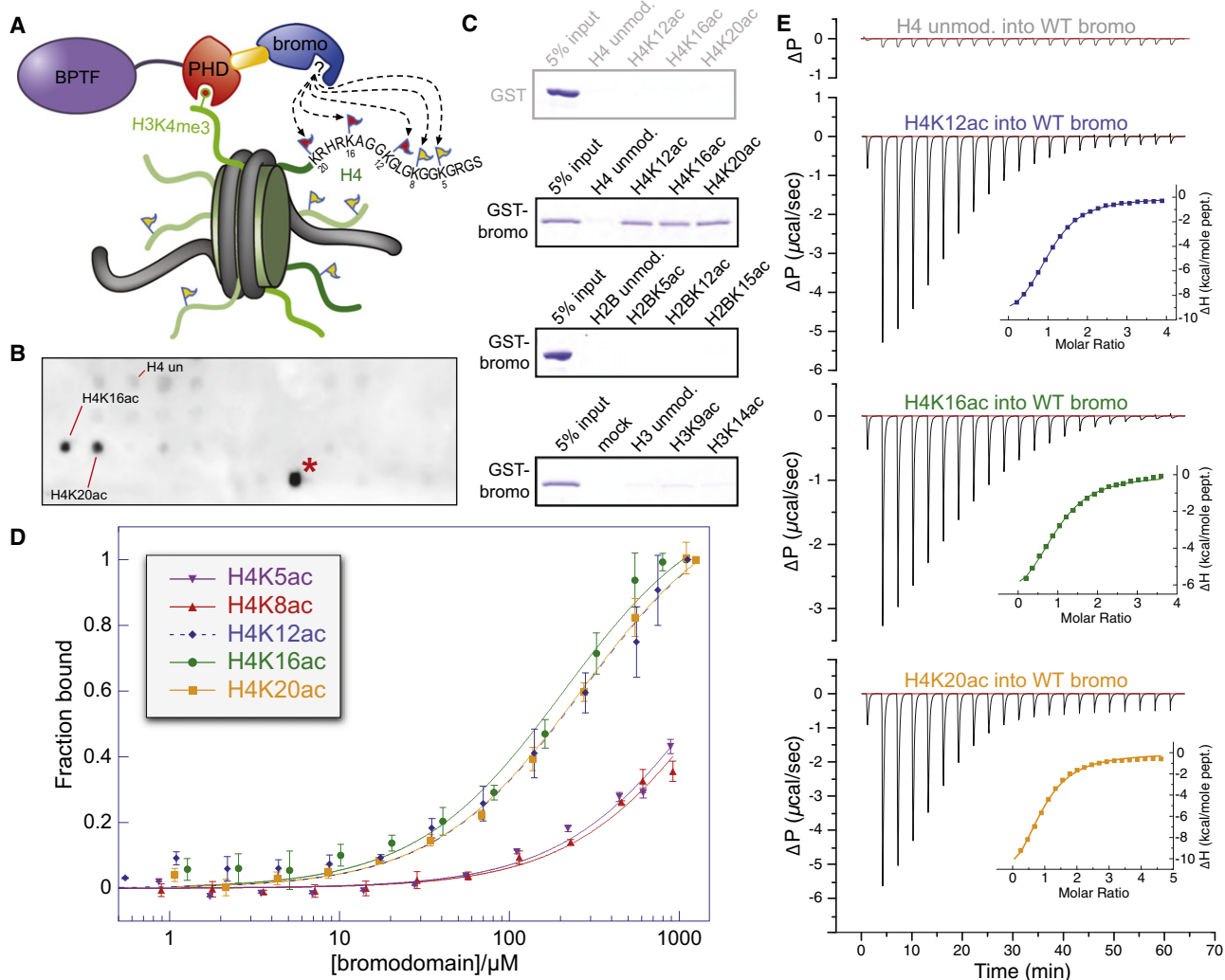


Figure 1. Systematic Characterization of Preferred Acetylated Histone Ligands for the BPTF Bromodomain

(A) Schematic representation of a putative bivalent nucleosomal interaction with the BPTF PHD-bromo module. The known point of contact (Li et al., 2006; Wysocka et al., 2006) is illustrated between the PHD finger (red) and H3K4me3 (red circle atop green histone tail), whereas the bromodomain (blue) interacts with an unknown acetylation site (flags on histone tails).

(B) A SPOT blot of an array containing all known human core histone acetylation sites on a modified cellulose scaffold probed with GST-tagged bromodomain. A representative SPOT blot (controls and remaining replicates, Figures S1A–S1C) displaying reproducible staining for H4 peptides (residues 11–25) acetylated on the ε amines of lysines 16 and 20, respectively (H4K16ac and H4K20ac). The staining of H2BK85ac (red asterisk) appears to be a peptide-HRP interaction, and there is no detectable binding between the bromodomain and this peptide in solution (Figure S1E).

(C) Peptide pull-down experiments with GST and GST-BPTF bromodomain (GST-bromo) against three peptide series indicated. Full gels with GST controls are available in Figure S1H.

(D) Fluorescence polarization anisotropy-based titration of the BPTF bromodomain against each of the indicated peptides (data are represented as mean ± SD).

(E) Isothermal titration calorimetry-based binding curves; the indicated H4 peptides are titrated into a solution of BPTF bromodomain (see Figure S1F for K_d values).

See also Figure S1.

annealed to an unmodified complementary DNA strand (Figure 2C). Given the distance spanned by the two peptide-binding pockets (~70 Å), this result suggests simultaneous binding by both modules. That the H3K4me3 peptide-duplex conjugate displayed little binding affinity was unexpected because the K_d for the PHD finger binding this peptide is ~100-fold tighter than that of the bromodomain binding H4K16ac (Li et al., 2006). Our

interpretation of this result is that the H3K4me3 peptide is sufficiently short such that the PHD finger incurs steric or electrostatic repulsion from the DNA conjugate upon binding, supported by the observation that this short peptide is bound effectively in the absence of DNA (Figure S2D). Remarkably, this impairment of PHD finger binding can be partially overcome by distal binding of the bromodomain to the same DNA ruler duplex.

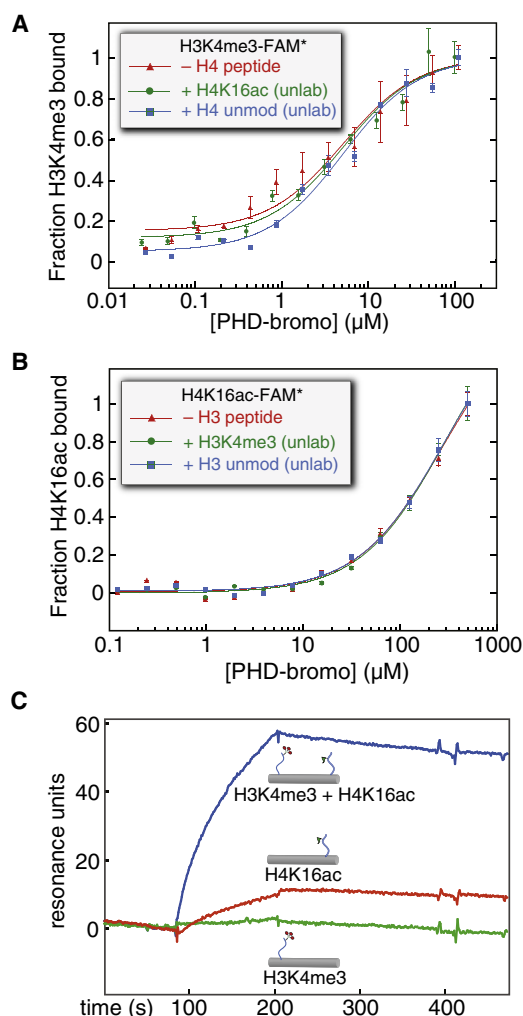


Figure 2. Is There Allosteric or Bivalent Cooperativity in Simultaneous Ligand Binding by the BPTF PHD-Bromodomain?

(A) The possible allosteric cooperative binding at the peptide level is examined by fluorescence polarization anisotropy using 100 nM fluorescein-labeled H3K4me3 peptide, with no additional peptide, excess unlabeled H4K16ac peptide (500 μM), or excess unlabeled H4 peptide without acetylation (500 μM). (B) The converse experiment with respect to (A). With unlabeled H3K4me3 in excess (20 μM, ~10-fold above PHD-H3K4me3 K_d) and fluorescein-H4K16ac (150 nM), protein is titrated and resulting fluorescence polarization anisotropy measured (expressed here as fraction bound).

(C) A dsDNA scaffold, selected for rigidity while retaining little predicted bending, was used to covalently install H3K4me3 (H3K4me3[1–8], green), H4K16ac (H4K16ac [12–20], red), or both peptides (blue) at specific positions by disulfide formation with cystamine-derivatized convertible dC nucleosides (Figure S2). All of these DNA-protein conjugates were immobilized in different flow channels via a single 3'-biotin linkage to a streptavidin-coated surface plasmon resonance chip at low density; untagged PHD-bromo was applied, and background binding was subtracted from an empty flow cell. Data are represented as mean \pm SD. See also Figure S2.

Encouraged that simultaneous binding of the PHD-bromodomain modules may provide an affinity enhancement, we sought to study these multivalent interactions on a more physiologically relevant substrate, the nucleosome.

To assess the consequences of bivalent nucleosome engagement, we sought to construct nucleosomes bearing the desired combinations of posttranslational modifications. To this end, we employed a histone semisynthesis approach of expressed protein ligation (EPL) (Muir, 2003; Shogren-Knaak and Peterson, 2004) to afford homogeneously modified histones that could be reconstituted with recombinant human core histones into octamers and then mononucleosomes on a strong positioning sequence (Figure S3 and Figure S4). GST-tagged BPTF PHD-bromodomain was immobilized on a glutathione resin and interrogated for binding to these radiolabeled mononucleosomes. A 2- to 3-fold enhancement of nucleosomal binding affinity was reproducibly observed for nucleosomes bearing both H4K4me3 and H4K16ac over mononucleosomes with only H3K4me3, whereas no binding was observed for the corresponding unmodified species (Figure 3A). Importantly, there was little detectable binding in this assay for nucleosomes acetylated only at H4K16—as might be anticipated from the ~100-fold K_d difference of the two discrete interactions extrapolated to an off-rate dominated binding measurement. To exclude GST-tag dimerization artifacts and surface effects, we performed a reciprocal experiment wherein nucleosomes are immobilized to a solid support and protein without the GST-tag is queried for nucleosome interaction by pull-down. The results are similar (Figure 3B and Figures S3K and S3L). We interpret the enhanced binding of doubly modified mononucleosomes to suggest that both marks may play a role in nucleosome-level binding, yet the PHD-H3K4me3 interaction is dominant.

Using this same assay, we revisited the question of specificity among the three candidate H4 acetylation marks that were previously identified in peptide-binding assays. Although selectivity between H4K12ac, H4K16ac, and H4K20ac peptides is limited, we wondered whether there might be additional binding constraints imposed by these marks when presented in a nucleosomal context. Though this assay is not sufficiently sensitive to detect bromodomain engagement of the acetylation marks in the absence of H3K4me3 binding (Figure 3C), again we observe a binding enhancement attributable to bivalent engagement only for H3K4me3 in combination with H4K16ac. Surprisingly, the other two acetylation marks (H4K12ac and H4K20ac), when paired with H3K4me3, do not display any binding enhancement beyond that due to H3K4me3 binding alone (Figure 3D). Despite similar peptide-level binding by the bromodomain, there is clear binding specificity at the mononucleosome level.

Does the BPTF PHD-bromo module preferentially bind to mononucleosomes, or do higher-order chromatin structures present the respective tails in a more productive spatial disposition for engagement? To begin to address this question, we constructed a series of dinucleosomal species via heteromeric DNA ligation of two mononucleosomes (McGinty et al., 2008; Zheng and Hayes, 2004) (see schematic in Figure 3E). Analogous pull-down experiments indicate that the dinucleosome composed of a nucleosome bearing both H3K4me3 and H4K16ac in position A and an unmodified nucleosome in position B is a modestly preferred binding partner of the PHD-bromodomain over the same two marks, each in adjacent nucleosomes assorted into either configuration (lane 6 versus 4 and 8 in Figure 3E and Figure S3N). Further, we do not observe simultaneous

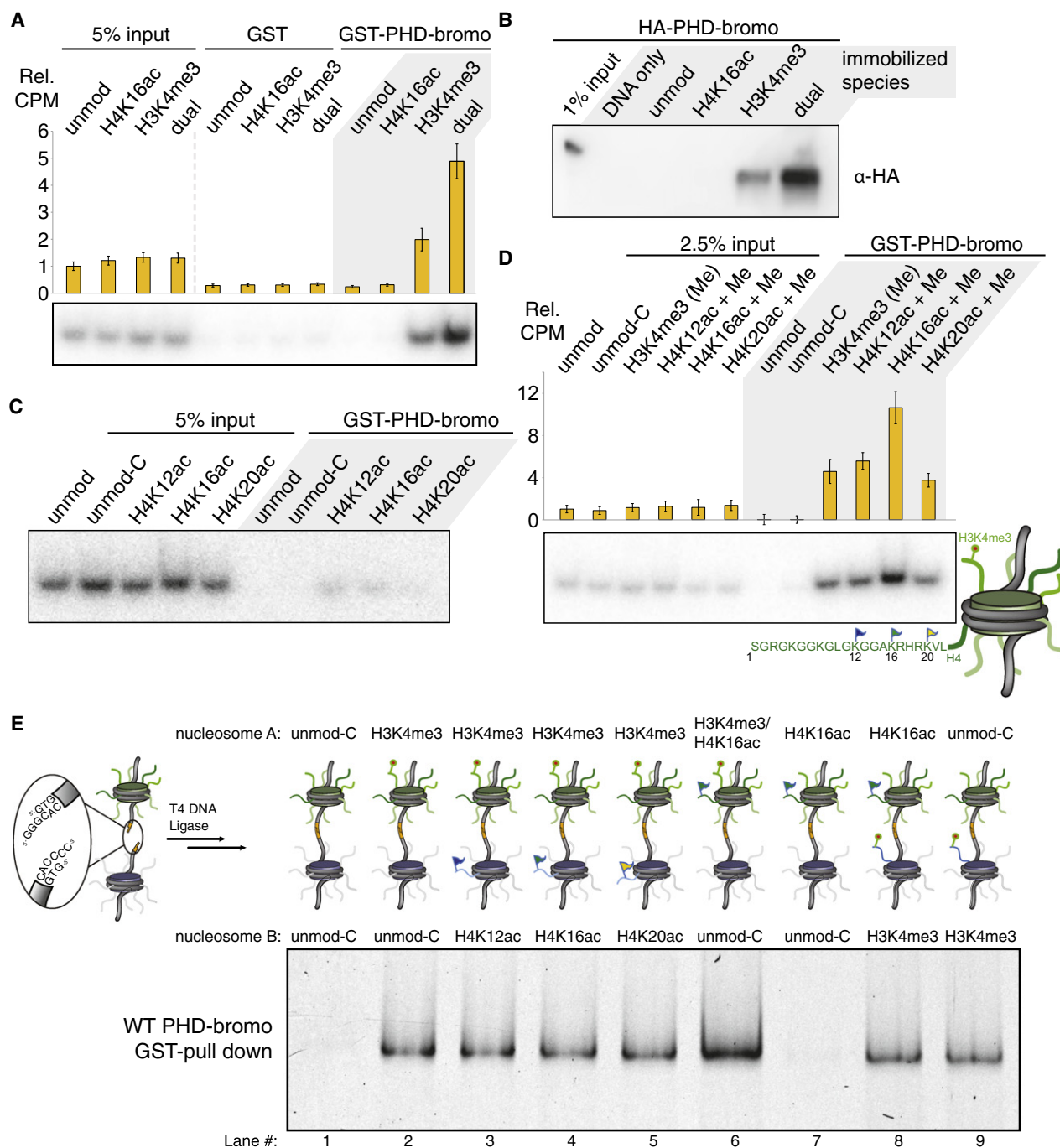


Figure 3. The BPTF PHD-Bromo Module Simultaneously Engages Two Heterotypic *trans*-Histone Marks in Nucleosomal Contexts

(A) GST pull-down of modified nucleosomes with semisynthetic histones produced by EPL. Nucleosomes (unmod, WT recombinant histones; H4K16ac modified; H3K4me3 modified; and dual, H4K16ac and H3K4me3 modified) pulled down with resin-bound GST or GST-BPTF PHD-bromo module protein are detected by autoradiography after native gel electrophoresis or scintillation counting normalized to indicated % input. Rel. CPM, yellow bars, represent mean \pm SD.

(B) The reciprocal experiment relative to Figure 3A. A western blot of HA-tagged PHD-bromodomain (without GST-tag) retained on streptavidin-immobilized mononucleosomes following extensive washing relative to 1% input.

(C) The nucleosomes bearing acetylated H4 alone do not display significant binding in the same GST-pull-down experimental format as described in (A). An additional control nucleosome species with H3T32C and H4R23C histones (unmod-C) serves as an unmodified nucleosome control that retains the cysteine ligation scars.

(D) In this experiment, all three H4 acetylation marks that are bound at the peptide level (Figure 1) are examined in combination with H3K4me3 at the nucleosome level as in (A). Data are represented as mean \pm SD.

binding to H3K4me3 and either of the other candidate H4 acetyl marks across two nucleosomes. Though this experiment does not exclude the possibility that higher-order nucleosome arrays or different spacing of linker DNA between nucleosomes A and B could produce more favorable tail orientations, our data suggest that the PHD-bromo module engages chromatin in an intra- rather than internucleosomal binding mode under the conditions examined.

To more precisely examine the intranucleosomal binding properties of the PHD-bromodomain, we next explored a panel of mutations that either abrogate the capacity of each domain to bind their respective substrates or perturb the spatial apposition of these two domains at the nucleosome level. An insertion of two amino acids (+QS) into the apparently rigid helix that links the PHD and bromodomains should rotate the two domains $\sim 200^\circ$ out of phase, assuming that the helix remains intact, changing the relative orientation of histone binding pockets (Figure 4A, inset). Neither perturbation of this helix nor mutations in the other domain substantially impact a given domain's intrinsic peptide binding capacity by FPA (Figure 4B). In the GST pull-down experiment, the W32E mutant most severely impaired BPTF association, whereas the F154A mutant displayed similar binding to the WT protein engaging the H3K4me3-modified nucleosome (Figure 4C). (For compact notation, all amino acid numbering here is relative to the start of the PHD finger at amino acid 2717 in the full protein.) Interestingly, a helix insertion mutant (+QS) is no longer able to bind doubly modified nucleosomes with both binding modules concomitantly reducing the amount of nucleosome retained to levels that are commensurate to the WT protein-binding nucleosomes bearing only H3K4me3. We further explored the role of this linker with extensive mutagenesis depicted schematically in Figure 4A insets. Perturbations of the linker were designed to extend the helix or introduce flexibility in this linkage with canonical helix-forming or helix-breaking residues (Chou and Fasman, 1978). Insertion near or replacement of several residues in the center of the helix uniformly impaired apparent bivalent interaction (Figure 4D). Taken together, these results suggest that the precise relative orientation of the two domains is a critical determinant of bivalent mononucleosome binding potential.

Structural Analysis Reveals Two Distinct Acetyl-Histone Binding Modes

As the mechanism of the composite selectivity in bivalent binding at the nucleosome level remained elusive, we wondered whether the molecular basis of H4ac peptide binding might provide meaningful insight. To this end, we solved high-resolution crystal structures of two different crystal forms of the BPTF bromodomain in complex with H4K16ac peptide—the preferred ligand of the PHD-bromodomain when combined with H3K4me3—and one structure of PHD-bromodomain in complex with H4K12ac peptide, representing a binding partner

that is not selected for in bivalent nucleosome binding, as a point of comparison (Figure 5 and Table S1). All of these data sets yielded interpretable electron density for acetyllysine and several flanking residues (Figures S5D–S5F). Beyond the well-documented bromodomain-acetyllysine contacts that are nearly identical in all three structures (Dhalluin et al., 1999; Mujtaba et al., 2007; Zeng et al., 2008), specific contacts are apparent in each structure that account for sequence context specificity.

The crystal form I H4K16ac-bromodomain complex reveals interactions that are analogous to those observed with the GCN5 bromodomain bound to the same mark ($C\alpha$ rmsd = 0.95 Å; Figure S5C). Remarkably, the H4 peptide orientation (N to C terminus) is inverted in our second structure (form II) relative to the first structure (Figures 5A, 5B, and 5F), despite nearly identical bromodomain conformation ($C\alpha$ rmsd = 0.52 Å). A similar reversal of peptide binding orientation has been previously noted with the PCAF bromodomain, albeit with two different H3 acetylation sites (Zeng et al., 2008). As a point of comparison to the two H4K16ac structures, we examined a PHD-bromodomain complex with ligand that does not contribute to bivalent binding of the PHD-bromodomain in combination with H3K4me3. The structure of the PHD-bromodomain in complex with H4K12ac displays a “reversed” peptide binding orientation similar to that observed in the form II complex (Figures 5B and 5C). However, the ordered region of the H4K12ac peptide is located atop the α B helix, more reminiscent of the peptide positioning in the form I H4K16ac complex (Figures 5A and 5F; for further details, see Supplemental Information).

Do both of these binding orientations contribute to the net affinity of the bromodomain for H4K16ac peptide? ITC was performed with bromodomain mutants designed to specifically perturb one of the two binding modes while leaving the other binding mode intact (Figures 5D and 5E). Although the binding of these mutant proteins to H4K16ac peptide was not strong enough to reliably quantify dissociation constants, residual binding affinity is apparent in the solution ITC measurements (compare ITC in Figures 5D and 5E with the H4 unmodified peptide binding in Figure 1E). Drastic alterations of contacts proper to the form II structure via point mutation of Trp 91 or Asp101 to alanine both severely erode but do not completely destroy binding (Figure 5E and Figures S5G and S5H). Selective disruption of interactions found only in the form I structure proved challenging, yielding conservative mutations that are more modest in their efficacy, V108A and Y147F. Nevertheless, these mutants demonstrate the solution binding relevance of this binding mode (Figure 5D and Figures S5G and S5I). From these data, we conclude that both bromodomain binding modes may play roles in the net affinity for H4K16ac peptide binding in solution. How the distinct molecular interactions in both the H4K12ac and H4K16ac complexes provide a plausible mechanism for nucleosomal H4 acetyl selectivity during bivalent binding of the nucleosome is addressed below (see Discussion).

(E) GST pull-down of hetero-dinucleosomes composed of two mononucleosomes indicated in positions A and B ligated together; each lane is labeled below numerically. The input dinucleosomes for this experiment are presented in Figure S3N.

See also Figure S3.

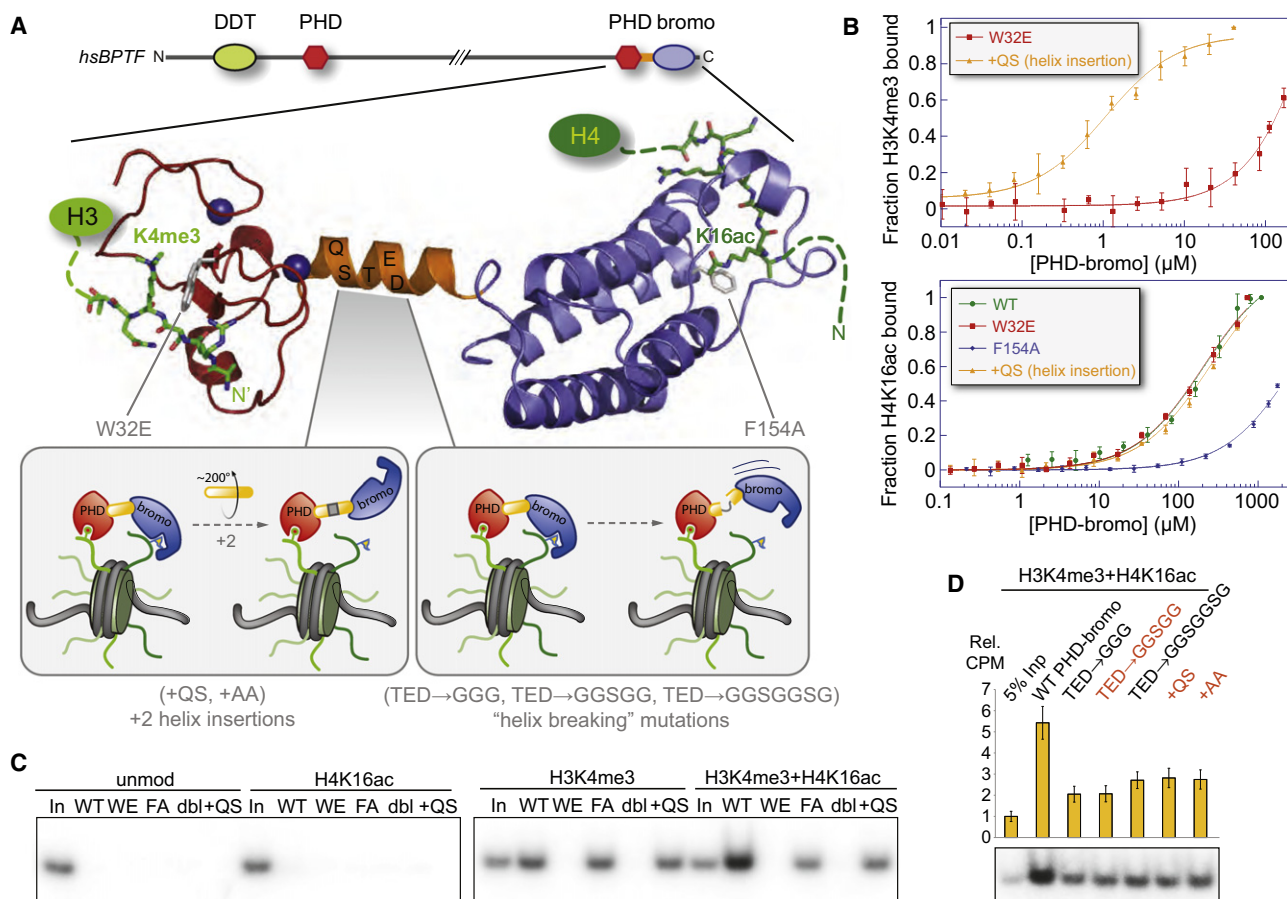


Figure 4. Querying the Roles of the PHD Finger, the Helical Linker, and the Bromodomain in Bivalent Nucleosome Binding via Mutagenesis

(A) A ribbon representation of the composite structure of the BPTF PHD-bromodomain module derived from superposition of the previously determined PHD-bromo in complex with H3K4me3 (Li et al., 2006) with the form I BPTF bromodomain H4K16ac complex (Figure 5A). The predicted domain structure of human BPTF shows the position of this module within the whole protein, colored as in Figure 1A, and mutations are indicated in gray. Inset panels schematically depict the anticipated consequences of a series of linker helix mutations.

(B) Mutations of the PHD-bromo module used to interrogate multivalent binding suggested by the structure assessed by FPA. (Top) A W32E mutation abolishes H3K4me3 binding without disrupting the PHD finger fold (Li et al., 2006; Peña et al., 2006; Ruthenburg et al., 2007a), whereas a two amino acid linker helix insertion (labeled +QS) leaves the H3K4me3 binding capacity intact. (Bottom) A F154A mutation, designed by analogy to previous bromodomain mutagenesis (Dhalluin et al., 1999), abolishes bromodomain binding of H4K16ac, whereas neither the +QS nor the W32E mutants disrupt binding. See Figure S1F for K_d values.

(C) Comparison of the WT GST-PHD-bromodomain (WT) to the series of mutant proteins in the same GST pull-down format as Figure 3. Mutants are labeled WE (W32E), FA (F154A), dbl (W32E + F154A), and +QS (a QS insertion after S58 in the bridging helix between the PHD) as depicted in (A), and 5% input is loaded for comparison (In).

(D) Mutations designed to break the α helix (residues 59–61 all mutated to glycine, TED → GGG; the same residues mutated to glycines in combination with "SG" or SGGS insertions, TED → GGSGG and TED → GGSGGG, respectively) are compared to mutations intended to extend the helix and thereby rotate the two domains out of phase (+QS or +AA inserted between and S58 and T59) in the same experimental format as (C). Mutations that effectively insert two amino acids into the linker helix are indicated in red.

Data are represented as mean \pm SD. See also Figure S4.

BPTF Colocalizes with Doubly Modified Nucleosomes in the Nucleus

The localization of BPTF to the *HOXA9* gene locus that is contingent upon H3K4 methylation mediated by the MLL complex has previously been established in HEK293 cells (Wysocka et al., 2006). Furthermore, MOF-mediated H4K16ac is highly enriched at the *HOXA9* locus in these cells (Dou et al., 2005). Native chromatin immunoprecipitation (ChIP) followed by qPCR on mononucleosome biased fragments recapitulates these trends and affirms more than an order of magnitude signal difference

for amplicons along this locus with the H4K12ac and H4K16ac antibodies (Figure 6A). To critically assess the relative import of each element in the BPTF PHD-bromo cassette for the localization of the full-length BPTF polypeptide to the *HOXA9* locus, we established HEK293 cell lines with stable and equivalent full BPTF expression (WT and several of the mutants described above; Figures S6A and S6B). The association of ectopically tagged BPTF protein with regions of the *HOXA9* locus, as assessed by ChIP (Figure 6B), largely recapitulates our in vitro findings within the modest dynamic range of the experiment. All

mutations diminish binding, suggesting that a minimally bivalent mode of nucleosomal engagement is important for BPTF recruitment or stabilization at this locus. Importantly, the +QS mutation disrupts localization to HOXA9. Thus, even in the context of full-length BPTF and presumably other NURF complex members, the precise orientation of the PHD finger and the bromodomain appears to be crucial for full binding both *in vitro* and *in vivo*. Given that the cell lines were constructed by stable integration of tagged BPTF into a genome with native BPTF expressed and that the NURF complex is dimeric in this subunit (Barak et al., 2003), complete loss of localization is not expected. In order to bypass this complication, we then restricted our ChIP-seq experiments to the BPTF PHD-bromodomain module.

Native ChIP followed by Illumina sequencing was performed to fully ascertain the genome-wide distribution of the H3K4me3, H4K12ac, and H4K16ac marks in this cell line and correlate them with the PHD-bromodomain localization (Figures 6C–6E). The latter data set was gathered via cross-linking ChIP from a tagged PHD-bromo expressing HEK293 cell line (Figure S6A). We detect numerous gene-proximal chromatin domains that bear significant peaks for H3K4me3 and each of the two acetylation marks examined; two examples are depicted in Figures 6C and 6D. Significant overlap between peaks of H3K4me3 and the tagged PHD-bromodomain was observed in a global sense. Although the number of clear peaks for the PHD-bromo is a much smaller set than the H3K4me3, 84% of these PHD-bromo peaks appear within 500 bp of an H3K4me3 peak (Figure S6C). As previously observed (Wang et al., 2008), the acetyl-specific ChIP-seq tracks are qualitatively more diffuse and less peak-like than the H3K4me3 signal, and consequently, peak calling relative to input was more challenging. Even so, the average tag densities differ in a locus-specific manner biased toward euchromatic regions, suggesting that the acetyl histone signal is meaningful (Figure S6D). Given that the PHD-bromo module colocalizes with a subset of H3K4me3 peaks (28%) and the broader distribution of acetyl marks, we would not expect very significant overlap in a global metagene analysis. Indeed, as depicted in Figure S6E, there is some overlap in the PHD-bromo and H3K4me3 average signal plotted for all genes normalized to 3 kb and very modest correlation with acetyl mark signal (Shin et al., 2009).

Although the PHD-bromo is not present at every H3K4me3 site, its presence appears to be more correlated with loci that also bear histone H4 acetylation. Plotting the average PHD-bromo tag count over the peak regions in the H4K16ac and H3K4me3 data sets, as well as where these two peaks intersect (within 150 bp), the apparent tag density is much higher for the PHD-bromo when H3K4me3 is combined with H4K16ac relative to either mark in isolation (Figure 6E). However, this also appears to be the case for the PHD-bromodomain plotted on intervals that are called peaks for both H4K12ac and H3K4me3. Taken together, these data suggest that the PHD-bromodomain tends to colocalize with H3K4me3 in regions that appear to have a reasonably high density of both H4K12 and H4K16 acetylation marks, particularly near TSS elements. The ChIP-seq data are consistent with the proposed role of both H3K4me3 and H4 acetylation in PHD-bromo recruitment, but there seems to be little distinction between the two H4ac

marks when examined by this method. This raises an important question regarding overlapping ChIP-seq peaks: do they actually represent coexistence of two given marks within a single nucleosome?

In order for the simultaneous bivalent binding of NURF described *in vitro* to be meaningful, mononucleosomes bearing both H3K4me3 and H4K16ac marks must exist in cells. To address this issue, we isolated high-purity mononucleosomes by sucrose gradient fractionation of MNase fragmented chromatin derived from HEK293 nuclei (Figure 7A and Figures S7A–S7F) (Mizzen et al., 1999). We then examined these purified nucleosomes for the coexistence of H3K4me3 with H4K16ac marks by coimmunoprecipitation relative to additional modifications and variants. There is a substantial pool of mononucleosomes bearing both modifications implicated in BPTF binding, H3K4me2/3 and H4K16ac (Figure 7B), whereas neither of these marks was found to reside in the same mononucleosomes as canonical repressive marks (H3K9me3 and H3K27me3). To exclude the possibility of off-target antibody recognition bias, we performed the reciprocal immunoprecipitation experiments, employing an α -H3K4me3 antibody for IP followed by staining for H4K16ac (Figure 7B, right). H3K4me3 antibodies did not robustly IP H4K12ac—another mark that the bromodomain is capable of binding at the peptide level (Figure 1)—or any other H4 acetylation mark. This finding suggests another possible source of selectivity: H4K12ac/H3K4me3 doubly modified mononucleosomes do not appear to be present in a detectable population (antibodies are not available to H4K20ac, the other histone mark that is bound effectively by the BPTF bromodomain at the peptide level; see Figure 1). However, we observed substantial co-occupancy of H3K4me3 and H4K20me2, consistent with the observation that > 80% of H4K20 is dimethylated at any given time, whereas the corresponding acetylation is not very abundant (Pesavento et al., 2008).

The analogous pull-down from the same highly purified mononucleosomal pools employing GST-tagged BPTF in place of antibodies again demonstrates preferential binding of the PHD-bromo module to H3K4me3- and H4K16ac-bearing nucleosomes (Figures 7C and 7D). Additional coexisting marks resembled the pattern observed in the mononucleosomal IPs. Consistent with our semisynthetic nucleosome experiments, the PHD-bromo module bound a greater quantity of H4K16ac mononucleosomes as compared to the bromodomain alone (Figure 7D), with similar resin loading levels (Figure S7F). We did not detect significant BPTF binding to H4K12ac-modified mononucleosomes under these conditions. This could reflect lower abundance of intranucleosomal H3K4me3 but may also be a function of reduced BPTF binding. In order to distinguish these two possibilities, we cultured cells in trichostatin A, a potent HDAC inhibitor that serves to enrich otherwise transient acetylation marks like H4K12ac (Pesavento et al., 2006); and despite substantial enrichment of the mark, we observed minimal binding to the PHD-bromo module (Figure S7H).

DISCUSSION

One explicit prediction of the histone code hypothesis is the combinatorial readout of multiple histone marks (Strahl and Allis,

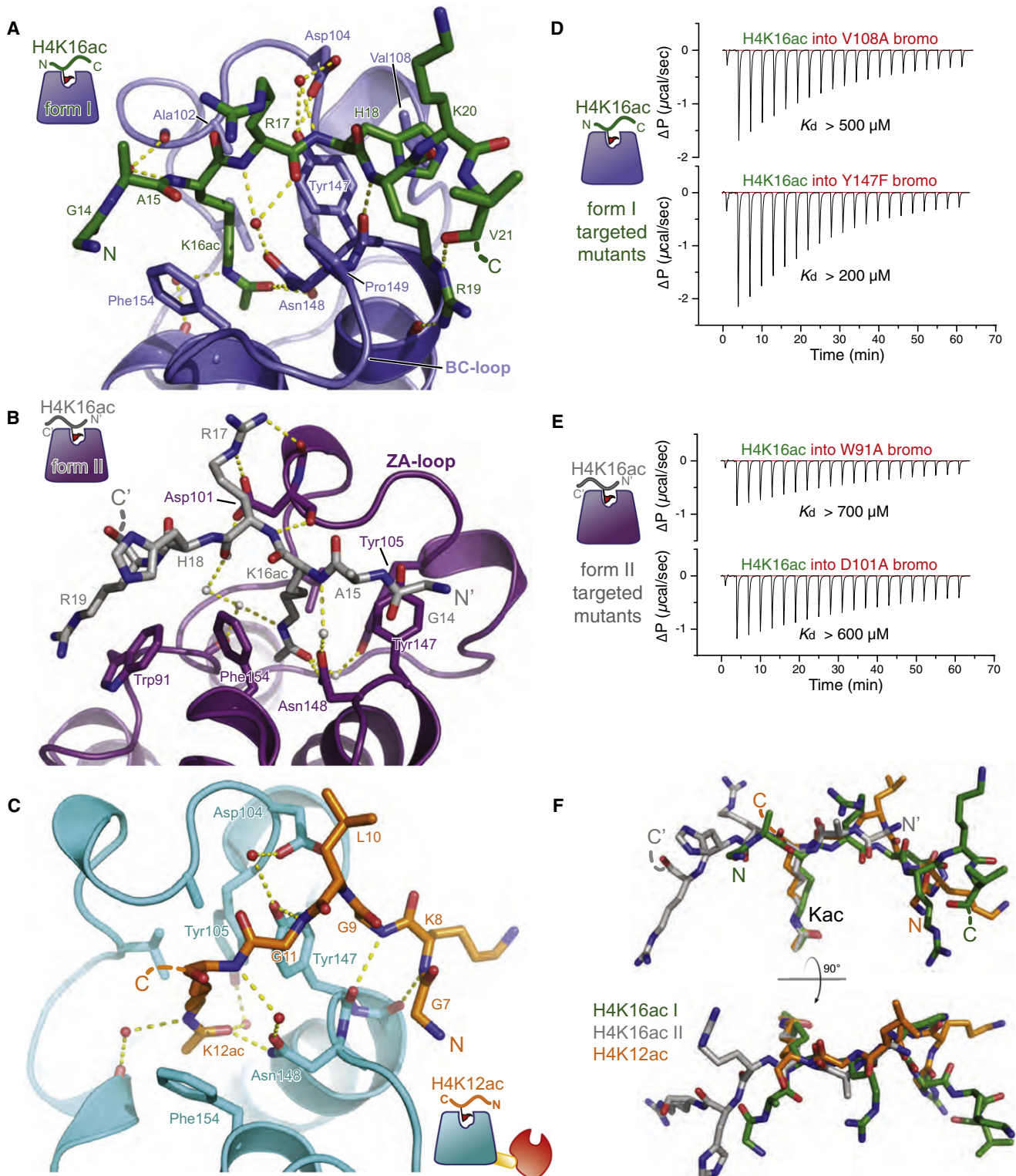


Figure 5. Structural Analysis of the BPTF Bromodomain Peptide Complexes

(A) The model derived from crystal form I (bromodomain in blue) with the apical binding site for the H4K16ac peptide (green) rendered in ribbons and sticks. Hydrogen bonds are displayed as yellow dashed lines.

(B) Interactions in crystal form II. The bromodomain is colored purple, and the bound H4K16ac peptide is depicted in gray.

(C) Interaction of the PHD-bromodomain in complex with H4K12ac peptide (peptide, orange; bromodomain, cyan).

2000), although experimental support for this prediction is lacking. Here, we present evidence for recognition of multiple heterotypic histone modifications simultaneously in a binding event that spans two different histone tails to establish nucleosome-level engagement contingent upon two discrete modifications. Of the three acetylated peptides with measureable bromodomain affinity, H4K16ac is an intuitively attractive BPTF binding partner. This mark is installed by the MOF acetyltransferase that may reside within the same MLL1 complex (Dou et al., 2005) that methylates H3K4 (Milne et al., 2002), the preferred binding partner of the proximal PHD finger (Li et al., 2006; Wysocka et al., 2006). The aggregate affinity of the PHD-bromo module for H3K4me3 and H4K16ac doubly modified nucleosomes is greater than that of the PHD and bromodomains alone yet more modest in magnitude than perhaps one would anticipate from discrete module-mark dissociation constants. Importantly, the bivalent nature of this interaction appears to effectively enhance the specificity of the bromodomain. Tethering of the PHD-finger to nucleosomal H3K4me3 appears to constrain the bromodomain to bind only H4K16ac, although at the peptide level, there is not much distinction in binding affinities for this mark relative to the two flanking H4 acetyl marks.

What is the molecular mechanism for this composite specificity? Notwithstanding the molecular basis of each domain's interactions with cognate peptides and the clear importance of the linker in permitting bivalent interactions, the precise molecular mechanism of this selectivity remains elusive. Our combined structural and mutagenesis studies with the BPTF bromodomain provide one potential explanation: the H4K16ac peptide has access to two alternate binding modes, whereas the H4K12ac may have access to only one of these peptide binding orientations. Modeling suggests that only the peptide orientation in the form I H4K16ac bromodomain complex structure will accommodate a reasonable H3K4me3 approach angle in a nucleosome (Figure S5J), whereas the binding mode in the crystal form II structure does not seem to be compatible with bivalent binding (Figure S5K). Using similar constraints, we are unable to model the PHD-bromodomain spanning H4K12ac and H3K4me3 that is consistent with binding orientations observed in the structures. Literal interpretation of this bivalent model brings the BPTF PHD-bromo module in close contact with DNA. Yet, inspection of protein surface electrostatics suggest that the association may not be this intimate; H3 tail flexibility could enable bivalent binding without engendering significant electrostatic repulsion from the nucleosomal DNA (Figure S5J, red arrow displays potential rigid body movement of PHD-bromo module away from the nucleosome). This model is consistent with the hydroxyl-radical footprint of the *Drosophila* NURF complex bound to a strongly positioned nucleosome; the region

of DNA near the pseudo-dyad at the duplex entrance/exit where the N-terminal H3 and H4 tails emerge from the octamer core is protected from cleavage (Schwanbeck et al., 2004). However, unambiguous delineation of the mechanism of H4 acetyl mark discrimination awaits the structural elucidation of the doubly modified mononucleosome in complex with the PHD-bromodomain.

How might this modest affinity gain be functionally important for the full NURF complex? It appears that every element of the bivalent nucleosome-binding interface described here is requisite for proper localization of the NURF complex to developmentally important loci in human cells. Yet in *Drosophila*, genetic deletions of a large portion of the C terminus of BPTF (including the PHD-bromodomain) present no developmental defects outside of gametogenesis (Kwon et al., 2009), and there are known DNA sequence-specific factors involved in NURF recruitment (Badenhorst et al., 2005; Tsukiyama and Wu, 1995; Xiao et al., 2001). In vertebrates, there are no analogous factors that are known to be involved in NURF recruitment, nor have clear DNA sequence elements related to NURF recruitment been identified. Here, the role of histone modifications in the recruitment or stabilization of NURF complex at target loci appears to play a more important role, as removal of PHD-bromo module results in severe homeotic, hematopoietic, and gut abnormalities that are not found in flies (Wysocka et al., 2006).

It is likely that the interplay of histone modification-specific interactions combined with other chromatin contacts determines the ultimate energetics and specificity in binding that culminates in genomic localization. Indeed, the bivalent interaction described here could be tetravalent in the context of the NURF complex, as there are two copies of BPTF in the NURF complex (Barak et al., 2003). Beyond the established nucleosomal contacts made by other NURF complex subunits—SNF2L likely has at least three DNA contacts (by analogy to ISWI) (Grüne et al., 2003; Schwanbeck et al., 2004), and RbAp46/48 binds the first helix of H4 (Verreault et al., 1998)—*Drosophila* BPTF (NURF301) bears three distinct nucleosomal interaction regions, only one of which may be attributed to the PHD-bromo module (Xiao et al., 2001). Specific interactions with the H4 tail, proximal to K16 and K20, seem to be essential for remodeling activity of NURF and other ISWI family complexes (Clapier et al., 2001; Hamiche et al., 2001; Shogren-Knaak et al., 2006).

Genome-level ChIP experiments have yielded a wealth of information about the localization of the H3K4me3 and H4K16ac histone marks; there are domains of significant overlap, particularly at active homeotic gene clusters. However, there is little data available that suggest what the absolute modification densities are at a given locus, so it is unclear to what extent spatially overlapping modification patterns described by

(D) ITC with BPTF bromodomain mutants designed to disrupt the form I binding mode (V108A and Y147F). Each of these mutations displays modest binding deficits comporting with their modest roles in the form I interface. Dissociation constants were outside of the accurately measurable range, so a lower limit of possible K_d is provided for qualitative comparison.

(E) Mutations to disrupt the form II binding interactions while leaving the form I binding mode intact. More substantial mutations, W91A and D101A, produce a more severe loss of affinity. For convenience of comparison, all ΔP scales are identical in scale.

(F) Binding conformations of peptides (colored as in previous panels) from each of the structures are compared by C α -superposition of their respective bromodomains.

See also Figure S5.

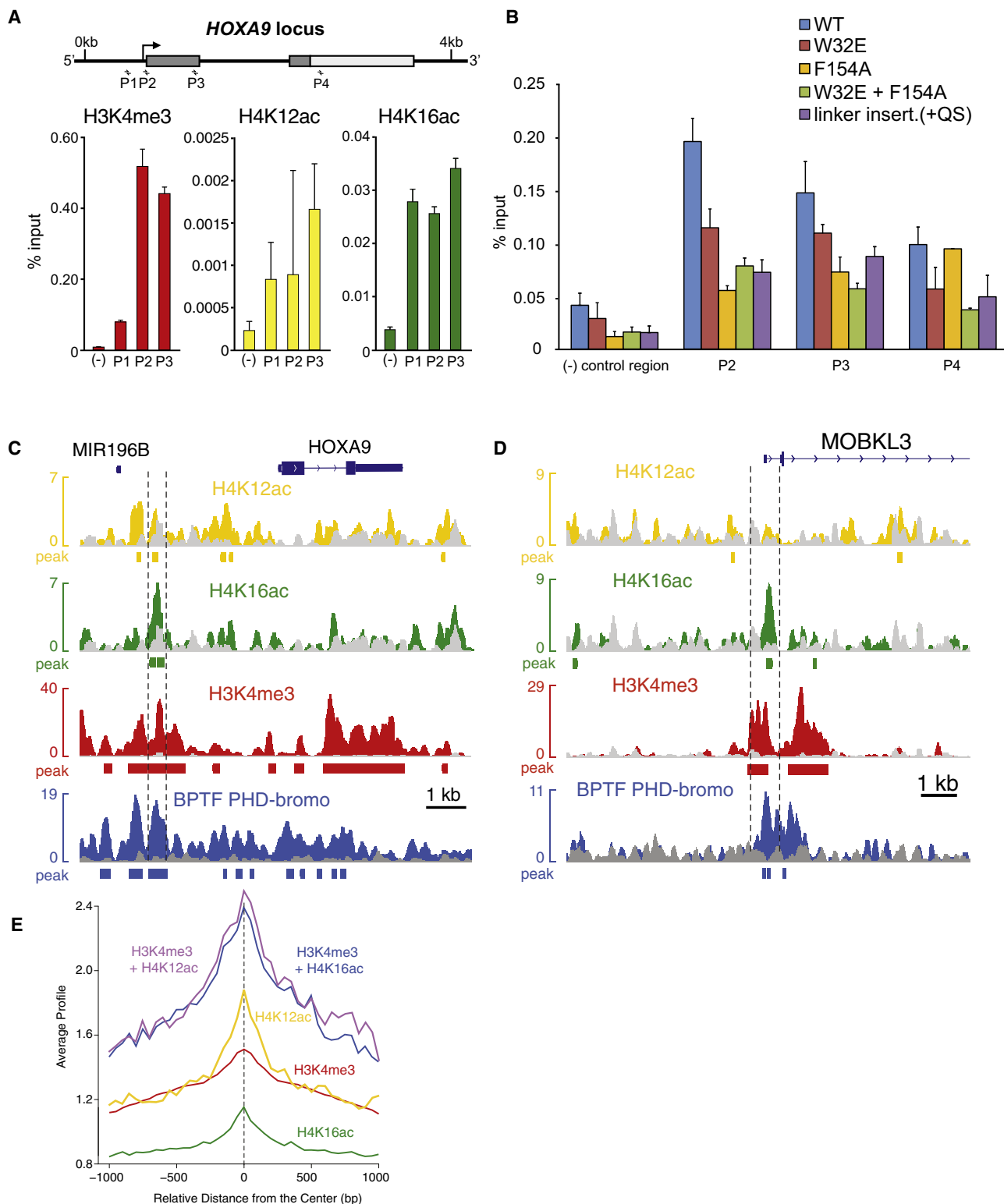


Figure 6. Bivalent BPTF Binding Is Important for Localization of the BPTF PHD-Bromodomain and Full NURF Complex

(A) Native ChIP comparison of H3K4me3, H4K12ac, and H4K16ac marks. Four primer sets were employed to interrogate the *HOXA9* locus (P1–P3, dark and light gray bars represent *HOXA9* exons, and an untranslated region, respectively) and a distal intergenic site ([–] control region). An average of three real-time PCR replicates of a representative experiment is displayed as a function of % input signal, with error bars reflecting \pm SD of PCR product threshold error among the replicates. For simplicity of *HOXA9* display, the gene structure annotation represents the Crick strand sense of the genome in this as well as (B) and (C).

ChIP-seq represent modifications that synchronously reside within a given nucleosome. By restricting the native chromatin queried to highly purified mononucleosomes, we provide compelling evidence for robust H4K4me3 and H4K16ac coexisting within a single nucleosome. In contrast, only modest coexistence of H3K4me3 and H4K12ac is detected by this method. This underscores a potential pitfall in interpreting ChIP-seq data: significant overlap of H3K4me3 with both of these acetyl marks, on average, may be observed across large genomic regions. Thus, apparent colocalization by this measure does not necessarily mean that two such marks actually coexist in the same mononucleosome.

The discovery of a significant pool of doubly modified H3K4me3/H4K16ac mononucleosomes is consistent with the biochemical identification of both enzymes that are responsible for installing these marks associating within the MLL1 complex in one preparation (Dou et al., 2005; Milne et al., 2002). The coexistence of these marks at MLL1-regulated loci by ChIP is also consistent with the notion that this distinct population of doubly modified mononucleosomes resides there. The clear coexistence of H3K4me3 and H3K79me2 marks in mononucleosomes was unanticipated, although others have noted this overlap by ChIP-seq (Wang et al., 2008). Interestingly, both H3K4me3 and H3K79me2 marks are downstream of H2B ubiquitylation (Briggs et al., 2002), and recent biochemical studies suggest direct stimulation of each responsible human methyltransferase by this ubiquitylation (Kim et al., 2009; McGinty et al., 2008).

Here, we have provided evidence not only for simultaneous recognition of two heterotypic histone marks in a binding event that spans two histone tails as they project from the nucleosome, but also potential resolution of a purported weakness in the histone code hypothesis (Strahl and Allis, 2000). If more than one module is capable of binding a given mark and each of these discrete modules resides in a different complex that transduces different downstream functional consequences, how can that mark itself have any unique information encoding potential (Becker, 2006)? For example, the “split personality” of the H3K4me3 mark may be engaged by Taf3 of the TFIID complex to increase transcription (Vermeulen et al., 2007) or the ING2-bearing mSin3a complex to silence certain genes upon DNA damage (Shi et al., 2006). How can complex localization in these diametrically opposed processes be governed by the same mark? Our work suggests that both the PHD finger and bromodomain binding modules, as well as their relative orientation, are important for the full BPTF binding and Hox gene localization of

the NURF complex. In this case, it is not the information content of interpreting a single mark that matters; rather, it is the combination of engaging a pattern of marks and perhaps other local chromatin features that ultimately dictates cellular localization. Our findings call attention to the histone code being more complex than the unique interpretation of a single mark and provide support for multivalent recognition of the chromatin polymer.

In addition to BPTF, there are 22 other polypeptides in the human proteome that display linked PHD fingers and bromodomains, some of which are remarkably similar to the BPTF-PHD module studied here (Ruthenburg et al., 2007b). Initial work with several of these proteins suggests that each domain may be important for chromatin association (Eberharter et al., 2004; Ragvin et al., 2004; Tsai et al., 2010; Zhou and Grummt, 2005). Investigation of whether similar bivalent interactions play a role in their nuclear function will be of interest. More generally, we anticipate that other examples of such combinatorial patterns being recognized by multivalent contacts at the level of single nucleosomes, oligonucleosomes, and chromatin territories will be important for numerous genomic transactions.

EXPERIMENTAL PROCEDURES

SPOT blots, peptide pull-downs, and fluorescence polarization anisotropy and ITC were performed essentially as described (Li et al., 2006; Nady et al., 2008; Wysocka et al., 2006). Details of recombinant protein production, X-ray crystallography, DNA-ruler assays, histone semisynthesis, and nucleosome reconstitution are available in the [Extended Experimental Procedures](#). In brief, recombinant histones were reconstituted into octamers with semisynthetic histones prepared via expressed protein ligation as well as complementary recombinant histones (Muir, 2003; Shogren-Knaak and Peterson, 2004); then, nucleosomes on a [³²P] end-labeled strong positioning sequence. Each nucleosome type was incubated with glutathione resin-immobilized GST-BPTF and washed five times for 45 min. The retained nucleosomal DNA was eluted from the resin, imaged by autoradiography of samples applied to native gels, and/or quantified by scintillation counting. In nucleosome MNase digestion was performed as a hybrid of previous conditions (Brand et al., 2008; Mizzen et al., 1999; O'Neill and Turner, 2003), with some modifications to the buffer conditions, and IPs were performed using conventional protocols. ChIP was performed according to established protocols or adaptations thereof; see [Extended Experimental Procedures](#) for details.

ACCESSION NUMBERS

Protein Data Bank model coordinates and structure factors have been deposited at the RCSB with the accession codes 3QZV, 3QZS, and 3QZT, representing the H4K12ac + PHD-bromo complex, the P2₁ crystal form of the

(B) xChIP of HA-tagged BPTF at the *HOXA9* locus from HEK293 cell lines that exhibit commensurate expression levels of the ectopically tagged constructs. ChIP signal (with primer sets P2–P4) of tagged WT protein expressing cell lines is compared to discrete cell lines bearing the tagged mutant proteins corresponding to mutations depicted in [Figure 4](#). Data are represented as mean ± SD.

(C) ChIP-seq data for the *HOXA9* locus, with the three histone modification tracks derived from nChIP-sequencing rendered in yellow, green, and red as labeled with input tag counts overlayed in gray on the same scale. On the same abscissal scale and register, the xChIP sequencing counts from the 3 × FLAG-tagged BPTF PHD-bromodomain are depicted in blue, with attendant input superimposed in gray. All tag counts are normalized by the factor (2 × 10⁷ / total mapped tags per track) and are unique. Below the continuous tag count graph, MACS peak-called regions relative to input for each sequencing track are depicted in rectangles of the same color.

(D) Another example of histone modification patterns and PHD-bromodomain binding, displayed as in the previous panel.

(E) Plot of average profile of the PHD-bromodomain at peak regions in the other data sets or intersects thereof. The average PHD-bromo signal is contoured on the regions that have MACS called peaks for each individual modification (colored as in C) or at loci with called peaks within the same 150 bp window for both H3K4me3 and H4K12ac data sets (purple) or H3K4me3 and H4K12ac data sets (blue).

See also [Figure S6](#).

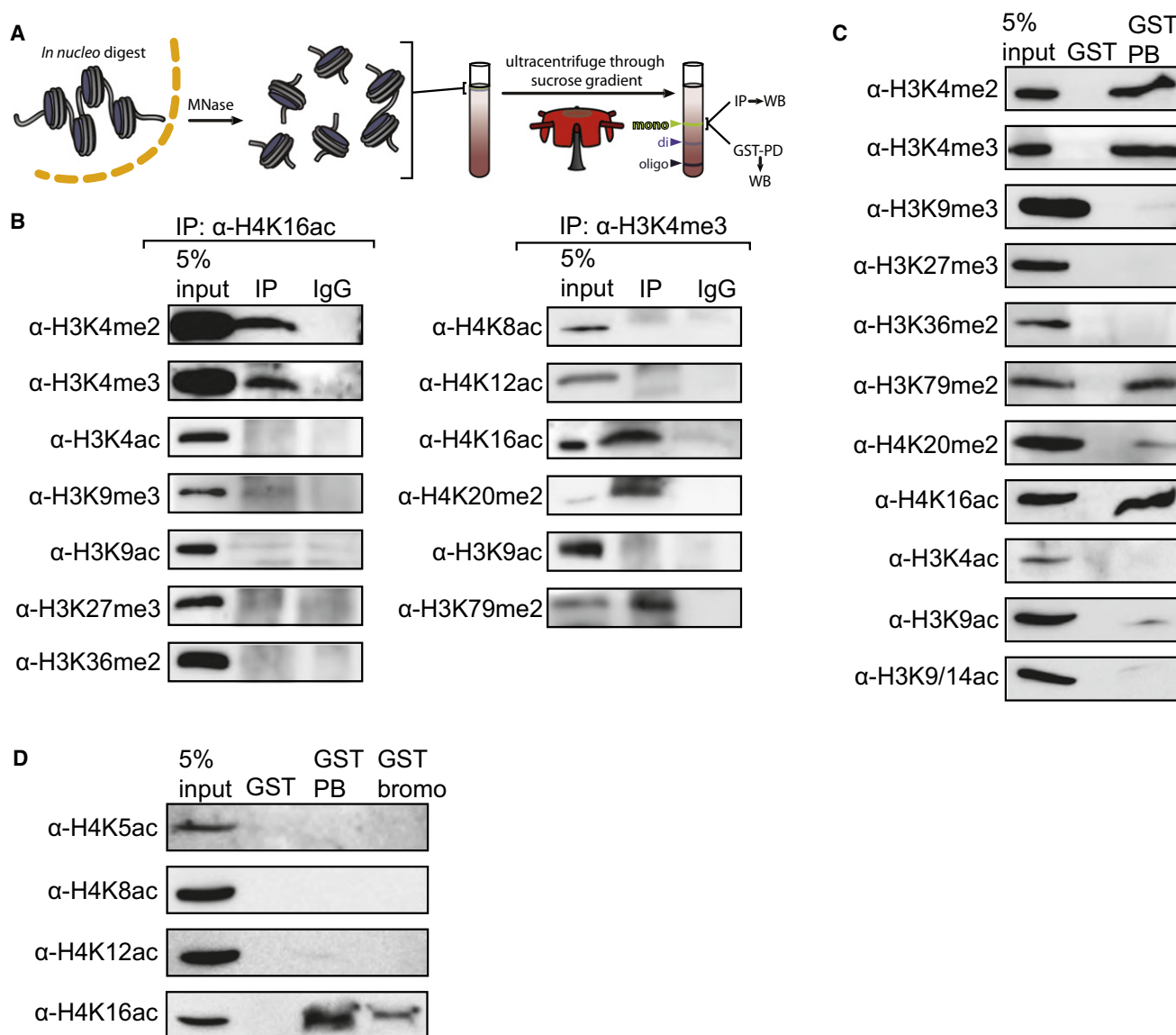


Figure 7. The BPTF PHD-Bromodomain Preferentially Engages a Native Population of H3K4me3 and H4K16ac Doubly Modified Nucleosomes

(A) Schematic representation of the experiments. Mononucleosome pools were isolated from in nucleo MNase digests and sucrose gradient ultracentrifugation. See Figure S5 for details.

(B) Coimmunoprecipitation and western blotting of highly purified mononucleosomes with the well-validated modification and sequence-specific histone antibodies indicated.

(C) Recombinantly produced GST-PHD-bromodomain (GST-PB) was used to pull down native mononucleosomes, and the associated material is compared to 5% of the input mononucleosome pool and GST alone for the ability to bind native nucleosomes contingent upon modification patterns.

(D) An additional pull-down with the GST-tagged bromodomain alone (GST-bromo) was performed alongside GST and GST-PB, and the bound material was probed by western blot against the four acetyl marks on the H4 tail for which there are antibodies available.

See also Figure S7.

H4K16ac + bromodomain complex, and the C2 crystal form of the H4K16ac + bromodomain complex, respectively.

SUPPLEMENTAL INFORMATION

Supplemental Information includes Extended Experimental Procedures, seven figures, and two tables and can be found with this article online at [doi:10.1016/j.cell.2011.03.053](https://doi.org/10.1016/j.cell.2011.03.053).

ACKNOWLEDGMENTS

We would like to thank the staff at beamline 24ID-C of the Advanced Photon Source at the Argonne National Laboratory and the staff at beamline X29 of the National Synchrotron Light Source at Brookhaven National Laboratory, supported by the US Department of Energy, for assistance with data collection. This work is based upon research conducted at the Northeastern Collaborative Access Team (NE-CAT) beamlines of the Advanced Photon Source and

the Macromolecular Crystallography Research Resource (PXRR) at the National Synchrotron Light Source, which are supported by the National Center for Research Resources at the National Institutes of Health. We would like to thank L. Liang for assistance in protein production and crystallization of BPTF H4 peptide complexes; H.A. Zebrowski for assistance in the preparation of the SPOT membrane; S.S. Yi of the Microchemistry and Proteomics Core at Memorial-Sloan Kettering Cancer Center for synthesis of peptides; Y. Wei of the Rockefeller Chemical Biology Spectroscopy center for use of their Biacore instrument; S. Yokoyama and H. Kurumizaka for an expression construct bearing codon optimized histone H4; K. Chiang for his 3_601_3_x32 repeat plasmid; M.Vila-Perello for HF cleavage of Boc-peptides; H. Dormann for HP1-chromodomain recombinantly produced protein; H. Yu of the Rockefeller Proteomics Core for MS assistance; C. Wu for the human BPTF cDNA; and L. Baker, F. Casadio, J. Denu, P.W. Lewis, K.-M. Noh, R.G. Roeder, R. Sadeh, D. Shechter, T. Swigut, G.G. Wang, and J. Wysocka for valuable discussions and scientific input. A.J.R. is supported by Irvington Institute Fellowship Program of the Cancer Research Institute, and R.K.M. is supported by an MSTP grant. This work was supported by a MERIT grant from the NIH and funds from The Rockefeller University to C.D.A., as well as funds from the Leukemia and Lymphoma Society and Starr Foundation to C.D.A. and D.J.P. D.J.P. is supported by funds from the Abby Rockefeller Mauze Trust and the Dewitt Wallace and Maloris Foundations, and T.W.M. is supported by an award from the NIH. D.J.P. is a consultant in GlaxoSmithKline's epigenetic programs.

Received: March 12, 2010

Revised: September 7, 2010

Accepted: March 30, 2011

Published online: May 19, 2011

REFERENCES

- Badenhorst, P., Voas, M., Rebay, I., and Wu, C. (2002). Biological functions of the ISWI chromatin remodeling complex NURF. *Genes Dev.* 16, 3186–3198.
- Badenhorst, P., Xiao, H., Cherbas, L., Kwon, S.Y., Voas, M., Rebay, I., Cherbas, P., and Wu, C. (2005). The *Drosophila* nucleosome remodeling factor NURF is required for Ecdysteroid signaling and metamorphosis. *Genes Dev.* 19, 2540–2545.
- Bai, X., Larschan, E., Kwon, S.Y., Badenhorst, P., and Kuroda, M.I. (2007). Regional control of chromatin organization by noncoding roX RNAs and the NURF remodeling complex in *Drosophila melanogaster*. *Genetics* 176, 1491–1499.
- Barak, O., Lazzaro, M.A., Lane, W.S., Speicher, D.W., Picketts, D.J., and Shiekhattar, R. (2003). Isolation of human NURF: a regulator of Engrailed gene expression. *EMBO J.* 22, 6089–6100.
- Basu, A., Rose, K.L., Zhang, J., Beavis, R.C., Ueberheide, B., Garcia, B.A., Chait, B., Zhao, Y., Hunt, D.F., Segal, E., et al. (2009). Proteome-wide prediction of acetylation substrates. *Proc. Natl. Acad. Sci. USA* 106, 13785–13790.
- Becker, P.B. (2006). Gene regulation: a finger on the mark. *Nature* 442, 31–32.
- Bernstein, B.E., Kamal, M., Lindblad-Toh, K., Bekiranov, S., Bailey, D.K., Huebert, D.J., McMahon, S., Karlsson, E.K., Kulbokas, E.J., III, Gingeras, T.R., et al. (2005). Genomic maps and comparative analysis of histone modifications in human and mouse. *Cell* 120, 169–181.
- Brand, M., Rampalli, S., Chaturvedi, C.P., and Dilworth, F.J. (2008). Analysis of epigenetic modifications of chromatin at specific gene loci by native chromatin immunoprecipitation of nucleosomes isolated using hydroxyapatite chromatography. *Nat. Protoc.* 3, 398–409.
- Briggs, S.D., Xiao, T., Sun, Z.W., Caldwell, J.A., Shabanowitz, J., Hunt, D.F., Allis, C.D., and Strahl, B.D. (2002). Gene silencing: trans-histone regulatory pathway in chromatin. *Nature* 418, 498.
- Changeux, J.P., and Edelstein, S.J. (2005). Allosteric mechanisms of signal transduction. *Science* 308, 1424–1428.
- Chou, P.Y., and Fasman, G.D. (1978). Empirical predictions of protein conformation. *Annu. Rev. Biochem.* 47, 251–276.
- Clapier, C.R., Längst, G., Corona, D.F., Becker, P.B., and Nightingale, K.P. (2001). Critical role for the histone H4 N terminus in nucleosome remodeling by ISWI. *Mol. Cell. Biol.* 21, 875–883.
- Dhalluin, C., Carlson, J.E., Zeng, L., He, C., Aggarwal, A.K., and Zhou, M.M. (1999). Structure and ligand of a histone acetyltransferase bromodomain. *Nature* 399, 491–496.
- Dou, Y., Milne, T.A., Tackett, A.J., Smith, E.R., Fukuda, A., Wysocka, J., Allis, C.D., Chait, B.T., Hess, J.L., and Roeder, R.G. (2005). Physical association and coordinate function of the H3 K4 methyltransferase MLL1 and the H4 K16 acetyltransferase MOF. *Cell* 121, 873–885.
- Eberharter, A., Vetter, I., Ferreira, R., and Becker, P.B. (2004). ACF1 improves the effectiveness of nucleosome mobilization by ISWI through PHD-histone contacts. *EMBO J.* 23, 4029–4039.
- Grüne, T., Brzeski, J., Eberharter, A., Clapier, C.R., Corona, D.F., Becker, P.B., and Müller, C.W. (2003). Crystal structure and functional analysis of a nucleosome recognition module of the remodeling factor ISWI. *Mol. Cell* 12, 449–460.
- Guenther, M.G., Levine, S.S., Boyer, L.A., Jaenisch, R., and Young, R.A. (2007). A chromatin landmark and transcription initiation at most promoters in human cells. *Cell* 130, 77–88.
- Hamiche, A., Kang, J.G., Dennis, C., Xiao, H., and Wu, C. (2001). Histone tails modulate nucleosome mobility and regulate ATP-dependent nucleosome sliding by NURF. *Proc. Natl. Acad. Sci. USA* 98, 14316–14321.
- Hamiche, A., Sandaltzopoulos, R., Gdula, D.A., and Wu, C. (1999). ATP-dependent histone octamer sliding mediated by the chromatin remodeling complex NURF. *Cell* 97, 833–842.
- Jacobson, R.H., Ladurner, A.G., King, D.S., and Tjian, R. (2000). Structure and function of a human TAFII250 double bromodomain module. *Science* 288, 1422–1425.
- Kim, J., Guermah, M., McGinty, R.K., Lee, J.S., Tang, Z., Milne, T.A., Shilatifard, A., Muir, T.W., and Roeder, R.G. (2009). RAD6-Mediated transcription-coupled H2B ubiquitylation directly stimulates H3K4 methylation in human cells. *Cell* 137, 459–471.
- Krishnamurthy, V.M., Estroff, L.M., and Whitesides, G.M. (2006). Multivalency in Ligand Design. In *Fragment-based Approaches in Drug Discovery*, W. Jahnke and D.A. Erlanson, eds. (Weinheim: Wiley-VCH), pp. 11–53.
- Kwon, S.Y., Xiao, H., Glover, B.P., Tjian, R., Wu, C., and Badenhorst, P. (2008). The nucleosome remodeling factor (NURF) regulates genes involved in *Drosophila* innate immunity. *Dev. Biol.* 316, 538–547.
- Kwon, S.Y., Xiao, H., Wu, C., and Badenhorst, P. (2009). Alternative splicing of NURF301 generates distinct NURF chromatin remodeling complexes with altered modified histone binding specificities. *PLoS Genet.* 5, e1000574.
- Landry, J., Sharov, A.A., Piao, Y., Sharova, L.V., Xiao, H., Southon, E., Matta, J., Tessarollo, L., Zhang, Y.E., Ko, M.S., et al. (2008). Essential role of chromatin remodeling protein Bptf in early mouse embryos and embryonic stem cells. *PLoS Genet.* 4, e1000241.
- Li, H., Ilin, S., Wang, W., Duncan, E.M., Wysocka, J., Allis, C.D., and Patel, D.J. (2006). Molecular basis for site-specific read-out of histone H3K4me3 by the BPTF PHD finger of NURF. *Nature* 442, 91–95.
- Li, B., Gogol, M., Carey, M., Lee, D., Seidel, C., and Workman, J.L. (2007). Combined action of PHD and chromo domains directs the Rpd3S HDAC to transcribed chromatin. *Science* 316, 1050–1054.
- McGinty, R.K., Kim, J., Chatterjee, C., Roeder, R.G., and Muir, T.W. (2008). Chemically ubiquitylated histone H2B stimulates hDot1L-mediated intranucleosomal methylation. *Nature* 453, 812–816.
- Milne, T.A., Briggs, S.D., Brock, H.W., Martin, M.E., Gibbs, D., Allis, C.D., and Hess, J.L. (2002). MLL targets SET domain methyltransferase activity to Hox gene promoters. *Mol. Cell* 10, 1107–1117.
- Mizzen, C.A., Brownell, J.E., Cook, R.G., and Allis, C.D. (1999). Histone acetyltransferases: preparation of substrates and assay procedures. *Methods Enzymol.* 304, 675–696.
- Morinière, J., Rousseaux, S., Steuerwald, U., Soler-López, M., Curtet, S., Vitte, A.L., Govin, J., Gaucher, J., Sadoul, K., Hart, D.J., et al. (2009). Cooperative

- binding of two acetylation marks on a histone tail by a single bromodomain. *Nature* **461**, 664–668.
- Muir, T.W. (2003). Semisynthesis of proteins by expressed protein ligation. *Annu. Rev. Biochem.* **72**, 249–289.
- Mujtaba, S., Zeng, L., and Zhou, M.M. (2007). Structure and acetyl-lysine recognition of the bromodomain. *Oncogene* **26**, 5521–5527.
- Nady, N., Min, J., Kareta, M.S., Chédin, F., and Arrowsmith, C.H. (2008). A SPOT on the chromatin landscape? Histone peptide arrays as a tool for epigenetic research. *Trends Biochem. Sci.* **33**, 305–313.
- O'Neill, L.P., and Turner, B.M. (2003). Immunoprecipitation of native chromatin: NChIP. *Methods* **31**, 76–82.
- Peña, P.V., Davrazou, F., Shi, X., Walter, K.L., Verkhusha, V.V., Gozani, O., Zhao, R., and Kutateladze, T.G. (2006). Molecular mechanism of histone H3K4me3 recognition by plant homeodomain of ING2. *Nature* **442**, 100–103.
- Pesavento, J.J., Bullock, C.R., LeDuc, R.D., Mizzen, C.A., and Kelleher, N.L. (2008). Combinatorial modification of human histone H4 quantitated by two-dimensional liquid chromatography coupled with top down mass spectrometry. *J. Biol. Chem.* **283**, 14927–14937.
- Pesavento, J.J., Mizzen, C.A., and Kelleher, N.L. (2006). Quantitative analysis of modified proteins and their positional isomers by tandem mass spectrometry: human histone H4. *Anal. Chem.* **78**, 4271–4280.
- Ragvin, A., Valvatne, H., Erdal, S., Arskog, V., Tufeland, K.R., Breen, K., ØYan, A.M., Eberharter, A., Gibson, T.J., Becker, P.B., and Aasland, R. (2004). Nucleosome binding by the bromodomain and PHD finger of the transcriptional cofactor p300. *J. Mol. Biol.* **337**, 773–788.
- Ruthenburg, A.J., Allis, C.D., and Wysocka, J. (2007a). Methylation of lysine 4 on histone H3: intricacy of writing and reading a single epigenetic mark. *Mol. Cell* **25**, 15–30.
- Ruthenburg, A.J., Li, H., Patel, D.J., and Allis, C.D. (2007b). Multivalent engagement of chromatin modifications by linked binding modules. *Nat. Rev. Mol. Cell Biol.* **8**, 983–994.
- Schwanbeck, R., Xiao, H., and Wu, C. (2004). Spatial contacts and nucleosome step movements induced by the NURF chromatin remodeling complex. *J. Biol. Chem.* **279**, 39933–39941.
- Shi, X., Hong, T., Walter, K.L., Ewalt, M., Michishita, E., Hung, T., Carney, D., Peña, P., Lan, F., Kaadige, M.R., et al. (2006). ING2 PHD domain links histone H3 lysine 4 methylation to active gene repression. *Nature* **442**, 96–99.
- Shin, H., Liu, T., Manrai, A.K., and Liu, X.S. (2009). CEAS: cis-regulatory element annotation system. *Bioinformatics* **25**, 2605–2606.
- Shogren-Knaak, M.A., and Peterson, C.L. (2004). Creating designer histones by native chemical ligation. *Methods Enzymol.* **375**, 62–76.
- Shogren-Knaak, M., Ishii, H., Sun, J.M., Pazin, M.J., Davie, J.R., and Peterson, C.L. (2006). Histone H4-K16 acetylation controls chromatin structure and protein interactions. *Science* **311**, 844–847.
- Strahl, B.D., and Allis, C.D. (2000). The language of covalent histone modifications. *Nature* **403**, 41–45.
- Taverna, S.D., Li, H., Ruthenburg, A.J., Allis, C.D., and Patel, D.J. (2007). How chromatin-binding modules interpret histone modifications: lessons from professional pocket pickers. *Nat. Struct. Mol. Biol.* **14**, 1025–1040.
- Tsai, W.W., Wang, Z., Yiu, T.T., Akdemir, K.C., Xia, W., Winter, S., Tsai, C.Y., Shi, X., Schwarzer, D., Plunkett, W., et al. (2010). TRIM24 links a non-canonical histone signature to breast cancer. *Nature* **468**, 927–932.
- Tsukiyama, T., and Wu, C. (1995). Purification and properties of an ATP-dependent nucleosome remodeling factor. *Cell* **83**, 1011–1020.
- Vermeulen, M., Mulder, K.W., Denissov, S., Pijnappel, W.W., van Schaik, F.M., Varier, R.A., Baltissen, M.P., Stunnenberg, H.G., Mann, M., and Timmers, H.T. (2007). Selective anchoring of TFIIID to nucleosomes by trimethylation of histone H3 lysine 4. *Cell* **131**, 58–69.
- Verreault, A., Kaufman, P.D., Kobayashi, R., and Stillman, B. (1998). Nucleosomal DNA regulates the core-histone-binding subunit of the human Hat1 acetyltransferase. *Curr. Biol.* **8**, 96–108.
- Wang, Z., Zang, C., Rosenfeld, J.A., Schones, D.E., Barski, A., Cuddapah, S., Cui, K., Roh, T.Y., Peng, W., Zhang, M.Q., and Zhao, K. (2008). Combinatorial patterns of histone acetylations and methylations in the human genome. *Nat. Genet.* **40**, 897–903.
- Wysocka, J., Swigut, T., Xiao, H., Milne, T.A., Kwon, S.Y., Landry, J., Kauer, M., Tackett, A.J., Chait, B.T., Badenhurst, P., et al. (2006). A PHD finger of NURF couples histone H3 lysine 4 trimethylation with chromatin remodelling. *Nature* **442**, 86–90.
- Xiao, H., Sandaltzopoulos, R., Wang, H.M., Hamiche, A., Ranallo, R., Lee, K.M., Fu, D., and Wu, C. (2001). Dual functions of largest NURF subunit NURF301 in nucleosome sliding and transcription factor interactions. *Mol. Cell* **8**, 531–543.
- Zheng, C., and Hayes, J.J. (2004). Probing core histone tail-DNA interactions in a model dinucleosome system. *Methods Enzymol.* **375**, 179–193.
- Zeng, L., Zhang, Q., Gerona-Navarro, G., Moshkina, N., and Zhou, M.M. (2008). Structural basis of site-specific histone recognition by the bromodomains of human coactivators PCAF and CBP/p300. *Structure* **16**, 643–652.
- Zhou, Y., and Grummt, I. (2005). The PHD finger/bromodomain of NoRC interacts with acetylated histone H4K16 and is sufficient for rDNA silencing. *Curr. Biol.* **15**, 1434–1438.